International Journal of GEOMATE, July, 2020, Vol.19, Issue 71, pp. 61 - 68
ISSN: 2186-2982 (P), 2186-2990 (O), Japan, DOI: https://doi.org/10.21660/2020.71.28369
Geotechnique, Construction Materials and Environment

INFLUENCE OF SEISMICITY DECLUSTERING ON GROUND MOTION PREDICTION EQUATIONS FOR CENTRAL SULAWESI SEISMIC REGION

*Sigit Pramono[1,3], Widjojo A.Prakoso[1], Supriyanto Rohadi[2], Dwikorita Karnawati[2], Edy Santoso[2], Aim Nurfajar[2]

[1]Civil Engineering Department, Universitas Indonesia, Indonesia; [2]Agency for Meteorology Climatology and Geophysics,Indonesia

*Corresponding Author, Received: 14 July 2019, Revised: 24 Feb. 2020, Accepted: 02 March 2020.

ABSTRACT: Central Sulawesi has very complex tectonic conditions, and therefore the earthquake hazard of the region needs to be carefully examined. One of the required components to develop such examination is regional ground motion prediction equations. This study describes the development of GMPEs for Central Sulawesi based on broadband velocitymeter and strong motion accelerations recorded by instruments managed by Indonesia geophysical authority temporarily since year 2015 and 2017. The accuracy of the resulting equations is examined further by performing the seismicity declustering processes using the Reasenberg method; the declustering process is to separate mainshock events from foreshock and or aftershock events. Note that, as the site class of the instrument locations is SD, the resulting GMPEs are only for SD sites. The resulting expected geometric mean peak ground acceleration from GMPE for all shocks (dependent seismicity) is similar to that for mainshocks only (independent seismicity), except for higher magnitude earthquakes due to the limited number of data available. The expected PGA values are examined further by comparing the values with the actual PGA from earthquakes in the Sausu Fault region, including the damaging 29 May 2019 earthquake. Depending on the earthquake magnitude, the GMPEs may overestimate or underestimate the PGA values. In addition, the residual analyses are conducted to examine trends of the expected PGA values.

Keywords: Sulawesi, Earthquake, Ground motion prediction equations, PGA, Declustering.

1. INTRODUCTION

Indonesia is a country with significant seismic activities, and Central Sulawesi is one of seismic regions. To perform seismic hazard analyses, ground motion prediction equations based on regional data are required, and to examine further the accuracy of the equations, seismicity declustering may be needed. This study briefly discusses the development of ground motion prediction equations for Central Sulawesi. Subsequently, the seismicity declustering processes are reported. The earthquake catalog used consists of earthquake records from instruments maintained by Indonesia Agency for Meteorology, Climatology, and Geophysics (BMKG) since year 2015.

Sulawesi has a K-shape island, and it is associated with the complex tectonic conditions in the center of Indonesia. These conditions are a result of interactions among three major tectonic plates in Southeast Asia. Central Sulawesi is a colliding location of two of the plates, and the region appears to have a rotating micro block contributingfurther to the complex tectonic setting.

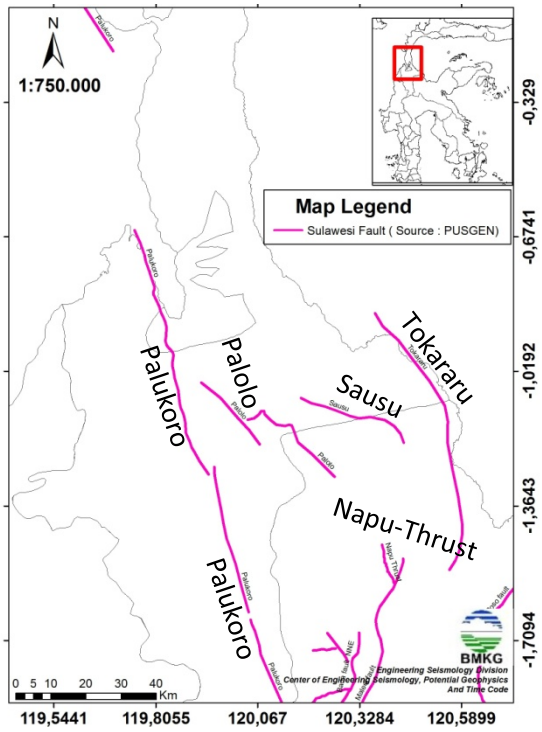


Fig. 1 Earthquake sources in Central Sulawesi [1]

Fig. 1 summarized the faults identified in [1]. The major fault is the left lateral strike slip Palu-Koro Fault; the 90° dip Palu and Saluki segments of the fault extend to about 75 km; the slip rate is estimated to be 20 – 40 mm/year, while the maximum magnitude is estimated from 6.8 to 6.9. The Palolo Fault is 60° dip normal fault extending to about 53 km. The Sausu Fault is a vertical strike-slip fault extending to about 30 km; the maximum magnitude is estimated to be 6.8. The Tokararu Fault and Napu Fault are is 45° dip thrust faults extending to about 80 km and 11 km, respectively. The maximum magnitude of Tokararu Fault is estimated to be 7.2. No slip rate estimates are available for the Palolo Fault, the Sausu Fault, and the Tokararu Fault. It is highlighted that the Palu-Koro Fault moved with a magnitude of 7.4 on 28 September 2018, causing a permanent sinistral offset up to about 5 m. The local site condition in Palu City identified by Pramono et.al [10] showed the deep of the engineering bedrock and site classification.

Fig.2 shows the earthquake epicenters within the BMKG Central Sulawesi earthquake catalog used in this study. As the catalog started in year 2015 and 2017, the earthquake data would not be exhaustive for the entire Central Sulawesi, and the proposed models represent initial models for the region. Also shown are the fault lines based on [1]. The size of the symbols represents the earthquake magnitude; the magnitude varied from 1.6 to 6.6.

2. DECLUSTERING METHODS

Seismicity consists of two parts: firstly, earthquakes that are independent and secondly, earthquakes that dependent on each other like aftershocks, foreshocks, or multiplets. Independent earthquakes are assumed to be mostly caused by secular, tectonic loading, in the case of seismic swarms, stress transients that are not caused by previous earthquakes. The second part corresponds to earthquakes triggered by static or dynamic stress changes, seismically-activated fluid, after-slip, etc. Hence by mechanical processes that are at least partly controlled by previous earthquakes. The process of separating earthquakes into these two classes is known as seismicity declustering.

The ultimate goal of declustering is therefore to isolate the class of background earthquakes, i.e. earthquakes that are independent of all preceding earthquakes. For large enough tectonic regions, the subset of independent earthquakes is expected to be homogeneous in time, i.e., a stationary Poisson process.

The fundamentals of the declustering methods have been developed from 1970s to 1980s by Gardner and Knopoff [2], Reasenberg [3], and Uhrhammer [4]. An example of the implementation of these methods was reported by Amini [5]. Gardner and Knopoff [2] introduced a procedure for identifying aftershocks within seismicity catalogs using inter-event distances in time and space; they provided specific space-time distances as a function of the mainshock magnitude to identify aftershocks, but they also encouraged readers to try out other

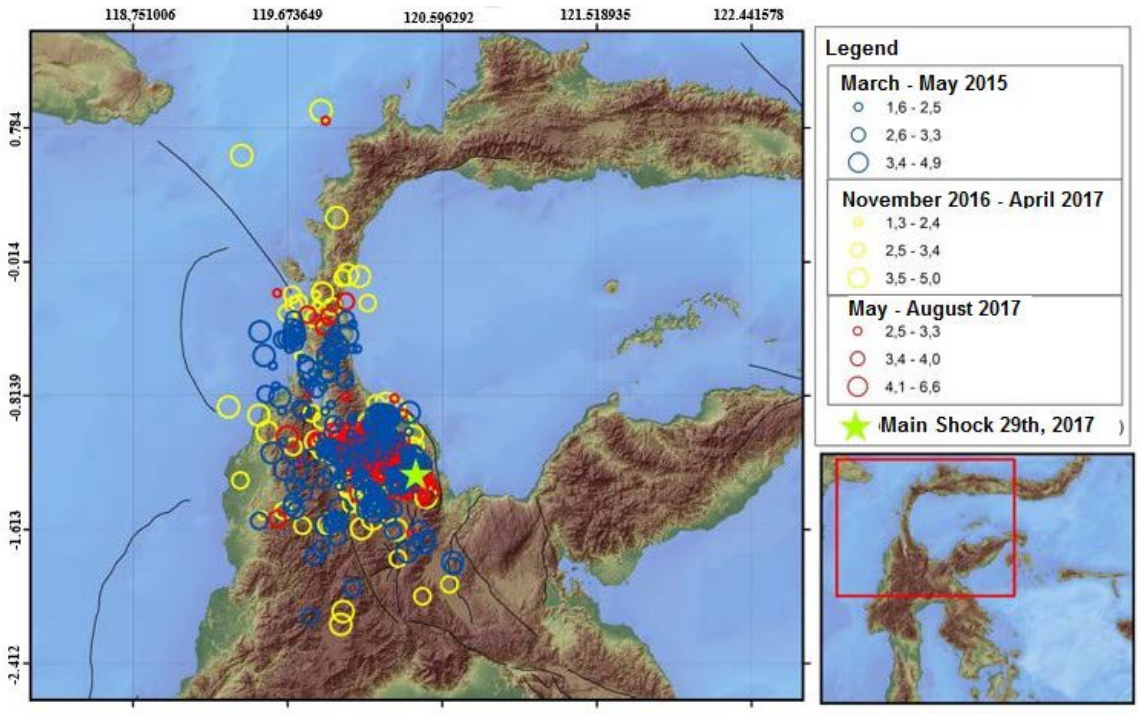


Fig.2. Historical seismicity map of Central Sulawesi

values. This method is known as a window method and is one of the simplest forms of aftershock identification. They ignored secondary and higher order aftershocks (i.e., aftershocks of aftershocks), if an earthquake C falls in the triggering windows of the two potential mainshocks A and B, then only the largest shock A or B is kept as the actual mainshock of C, regardless of the possibility that C might be significantly closer in space and time to the other shocks. They also did not consider fault extension for larger magnitude earthquakes by assuming circular spatial windows. Aftershocks are identified according to their proximity to large earthquakes in the dimensions of distance L(M) and time T(M)). When an earthquake data set is to be decluster, a least upper bound (LUB) or envelope to T (M) data is in the form of an equation:

$$\text{Log}\,(T) = a_1 M + b_1 \quad (1)$$

When all aftershock sequences have a T (M) value, the zone for aftershocks is estimated from Magnitude-length M (L) data, and then the upper bound value of the relationship is,

$$\text{Log}L = a_2 M + b_2 \quad (2)$$

The minimum upper limit is the window {T(M), L(M)} which is applied to an earthquake catalog. First of all, earthquake events in a catalog will be classified according to the distance L (M) and time T (M).

Reasenberg [3] introduced an algorithm method for identifying aftershocks by linking earthquakes to clusters according to spatial and temporal interaction zones. if A is the mainshock of B, and B the mainshock of C, then all A, B and C are considered to belong to one common cluster. When defining a cluster, only the largest earthquake is finally kept to be the cluster's mainshock. Earthquake clusters thus typically grow in size when processing more and more earthquakes. This method is based on the previous work of Savage [6]. The spatial extent of the interaction zone is chosen according to stress distribution near the mainshock, Reasenberg [3] spatial interaction relationship is defined by the threshold. (Molchan and Dmitrieva [7]).

$$\text{Log d (km)} = 0.4M_0 - 1.943 + k \quad (3)$$

Where k is 1 for the distance to the largest earthquake and 0 for the distance to the last one. The temporal extension of the interaction zone is based on Omori's law. All linked events define a cluster, for which the largest earthquake is considered the mainshock and smaller earthquakes are divided into foreshock and aftershocks.

Uhrhammer [4] using a method corresponding to aftershocks with catalog seismicity using a time window that uses distance radius and time window. Where the formula is :

$$R = 15 + \exp(-1.024 + 0.804M_m) \quad (4)$$

$$t_{win} = 60 + \exp(-2.87 + 1.235M_m) \quad (5)$$

where r is distance, t_{win}: time window period, and M_m:mainshocks magnitude.

The presumption of scale-independence for complete local earthquake catalogs is attributable, not to a universal process of self–an organization leading to feature large earthquake, but to the universality of the process that produces aftershocks, which dominate complete catalogs Knopoff [8]. In each region show, the complex seismicity condition depends on the potential source. So that the quality selected of seismicity to represent the energy source released is needed to be determined clearly. This basic formula has considered site classification issued. The basic functional form is the following:

$$log(Y) = \alpha + \text{b}(M) + \text{c}\log(R) \pm \sigma_{logY} \quad (6)$$

with Y: peak ground acceleration, M: local magnitude, R: Joyner–Boore distance or the epicentral or hypocentral distance, when the fault geometry is unknown (generally when M<5). For α, b, and c are the constant variables, and $\sigma_{logY}$is the deviation value for calculated value. This study used basic equation model adopted by Sharma et al. [9] to develop GMPE Himalaya.

3. DATA

This study used the BMKG Central Sulawesi earthquake catalog, compiling data recorded from the Indonesia National Strong Motion Network in 2015 (Phase 1), the Broadband for Ambient Network Tomography Indonesia-Australia (Phase 1), and the 9-month-long temporary strong motion network (Phase 2) in 2017. The duration of these phases was not the same. In addition, five (5) strong motion instruments were deployed in Balane, Tingede, Pandanjase, Kabonane, and Duyu. The strong motion instrument distribution is shown in Fig. 3. It is noted that, as the catalog started in year 2015 and 2017, the earthquake data would not be exhaustive for the entire Central Sulawesi.

The geotechnical site classes of the instrument locations varied. However, in this study, only locations with site class D (V_{s30} = 175 – 350 m/s) were considered. The BMKG stations with site class SD include Palu Station (SLPI), Tinggede Station (TDSI), and Kebonane Station (KNSI).

Fig. 4 shows the distribution of epicenters of the BMKG Central Sulawesi earthquake catalog used in this study. The epicenters are predominantly located in the region of Palolo Fault and Sausu Fault. Fig. 4a presents the distribution of all epicenters of the catalog (hereinafter called "dependent" data). The catalog was then declustered using the Reasenberg method [3]; Fig. 4b presents the resulting epicenter distribution (hereinafter called "independent" data). It is highlighted that Fig. 4b indicates the epicenters of the mainshocks of the region. By comparing Figs. 4a and 4b, one could see that the number of independent data(e.g., mainshocks) is much less than that of dependent data. For this reason, a more advanced analysis (e.g., [11]) could not be performed, and the same basic model is used for both "dependent" and "independent" models.

It is noted that this network recorded the damaging M_W = 6.6 Poso earthquake of main shock on 29th May 2017 as marked by a red star symbol on Fig. 4.The source of this earthquake was associated with a local active fault near the SausuFault, 39 km northwest of Poso City. The mainshock was followed by a series of aftershocks with varied magnitudes less than 6 (Fig. 4a). Three BMKG permanent stations recorded well the ground motion of this event.

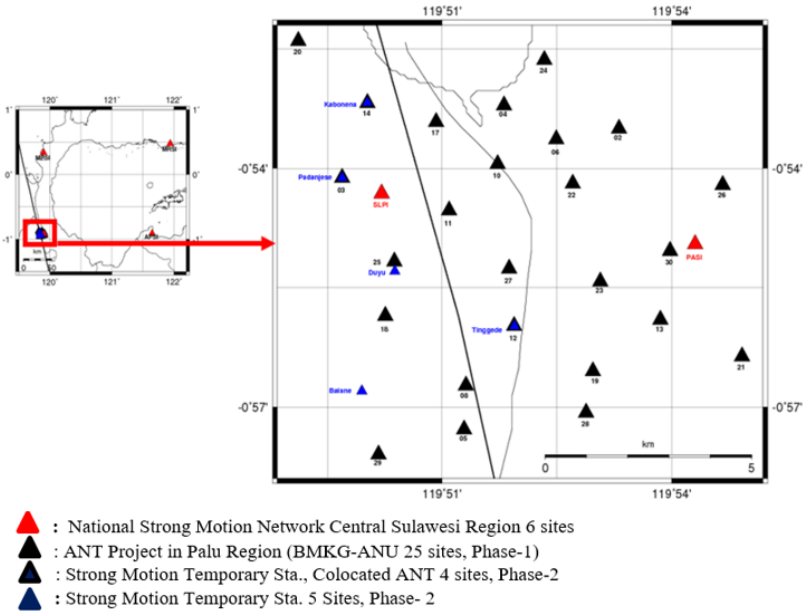
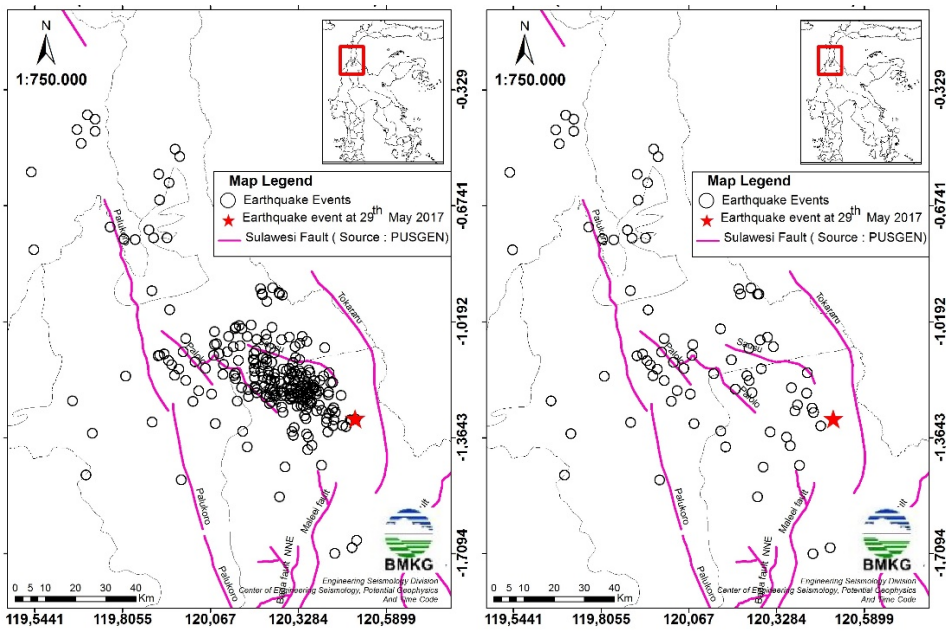


Fig.3 Strong motion instrument distribution



a) b)

Fig.4 Seismicity map: a) dependent events and b) independent events

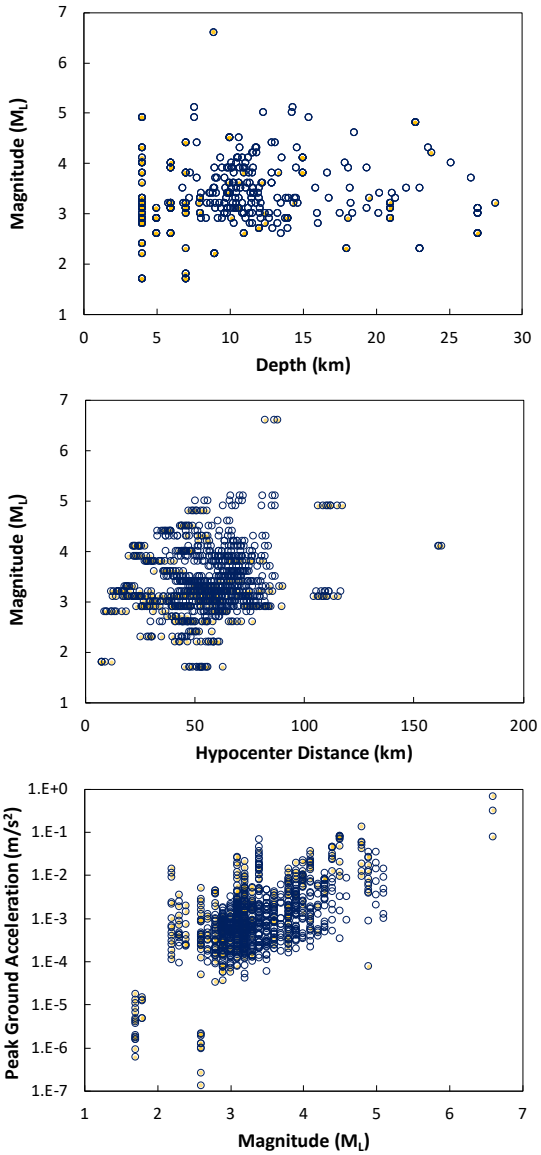


Fig.5 Central Sulawesi BMKG earthquake catalog: earthquake magnitude,hypocenter depth and distance, and geometric mean peak ground acceleration

Table 1. Constant values for GMPE

b_1	b_2	b_3	b_4	SD of τ
Constant values for dependent events				
-3.251	0.786	1.392	-19.409	0.076
Constant values for independent events				
-4.564	0.973	0.935	-14.825	1.083

Fig. 5 presents the earthquake magnitude, hypocenter depth and distance, and geometric mean PGA of the BMKG Central Sulawesi earthquake catalog. The number of dependent data is 1,021 data (void marker), while the number of independent data is 473 data (filled marker). The earthquake magnitude varied mostly from about 2.0 to about 5.0, with a very few less than 2.0 and great than 6.0. The hypocenter depth varied predominantly from 4 km to 15 km, while the hypocenter distance varied predominantly from 30 km to 80 km. The PGA as expected tends to increase with increasing earthquake magnitude. However, for a given magnitude, the range of PGA could be very significantly, up to two (2) logarithmic cycles.

4. RESULTS AND DISCUSSION

4.1 Ground Motion Prediction Equations

A ground motion prediction equation (GMPE) is an equation to determine the expected ground motion at a site due to an earthquake event. The ground motion would be influenced by the earthquake source, the wave path, and the local site effect. In this study, the general functional form of the GMPE is as follows:

$$\log A = b_1 + b_2 M - b_3 log \sqrt{{R_{Hyp}}^2 + {b_4}^2} + b_5 S + b_6 H + \tau \quad (7)$$

in which M: either M_W or M_L to represent low to moderate earthquake magnitude, R_{Hyp}: distance from earthquake hypocenter to site (km), S: effect of site class, H: type of fault mechanism, and τ: standard error. The GMPE output A could be the geometric mean peak ground acceleration (PGA) (m/s^2) or the 5% damped absolute acceleration response spectra (S_a,m/s^2) for higher structural natural periods. In this study, the variable S was set to zero as all data have site class SD, and H was set to zero as the GMPE was developed for earthquake sources. The mean of τ was set to zero, while the standard deviation (SD) of $\tau$was analyzed as well. The GMPE output considered is only the geometric mean PGA.

The BMKG Central Sulawesi earthquake catalog was examined further by performing multi-variate statistical analyses of the geometric mean PGA (i.e., geometric mean of north-south PGA and east-west PGA), both for dependent and independent data sets. The resulting constants b_1 through b_4, as well as SD of τ, for both data sets are summarized in Table 1.

Fig. 6 shows the expected geometric mean peak ground acceleration for different earthquake magnitude (2.0 to 7.0) for dependent and independent seismicity. It is noted that the lines for earthquake magnitude of 7.0 are different from the others to note that there were no actual data with magnitude greater than 7.0 used in the GMPE

development. In general, there are differences between the expected PGA for dependent and independent seismicity. The difference is the most pronounced for earthquake magnitudes of 6.0 and 7.0; this is possibly due to the lack of data with magnitude greater than 7.0.

The GMPEs for dependent and independent seismicity are examined further by comparing the resulting expected geometric mean PGA to the actual geometric mean PGA, as shown in Fig. 7. All earthquake events from Sausu Fault were used in the examination; the location of Sausu Fault is shown in Fig. 1.

Fig. 7a shows that the expected PGA values from both GMPEs appear to be well correlated to the observed strong motion data with magnitude between 2.4 and 3.0 (28 earthquake events). However, for magnitude less than 2.0 (two earthquake events), the GMPEs tend to overestimate the expected PGA values; this is possibly due to the lack of data with magnitude less than 1.5.

Fig. 7b shows that the expected PGA values tend to be higher than the observed strong motion data with magnitudeof 3.1 – 3.5 (66 earthquake events) and 3.6 – 3.9 (31 earthquake events). Fig. 7c shows that the expected PGA values tent to be higher rather significantly than the observed strong motion data with magnitude of 4.1-4.5 (21earthquake events) and 4.6-5.0 (3earthquake events).

Fig. 7d shows that the expected PGA values are greater than the observed strong motion data with magnitude of 5.1 (two earthquake events). Fig. 7e shows that the expected PGA values for dependent seismicity fit the observed strong motion data with magnitude of 6.6 (one event). However, the values for independent seismicity are greater than the observed data.

4.2 Residual Analysis

The residual analysis was performed to examine any trends of the results of multi-variate statistical analyses of strong motion geometric mean peak ground acceleration. Residuals are defined as the logarithmic ratio of the expected PGA to the actual PGA. The results of residual analysis against the hypocenter distance are shown as Fig. 8. A positive residual value means that the expected PGA is greater than the actual PGA (i.e., expected PGA overestimated).

Figs. 8a through 8c (earthquake magnitude up to 5.0) show that the distribution of residuals is relatively similar, predominantly from -1.0 to 1.0. Figs. 8d and 8e show that the residuals tend to be positive, indicating the overestimated expected PGA. Furthermore, the residuals for dependent GMPE tend to be lower than those for independent GMPE. For Poso Earthquake M = 6.6, the residuals for dependent GMPE varied from -0.5 to 0.6, while those for independent GMPE are all positive.

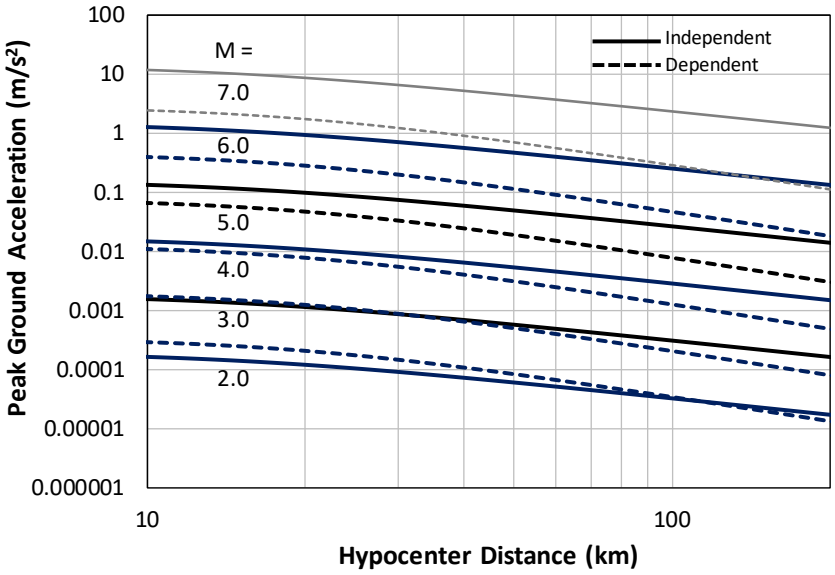


Fig.6 Expected geometric mean peak ground acceleration for different earthquake magnitude for dependent and independent seismicity

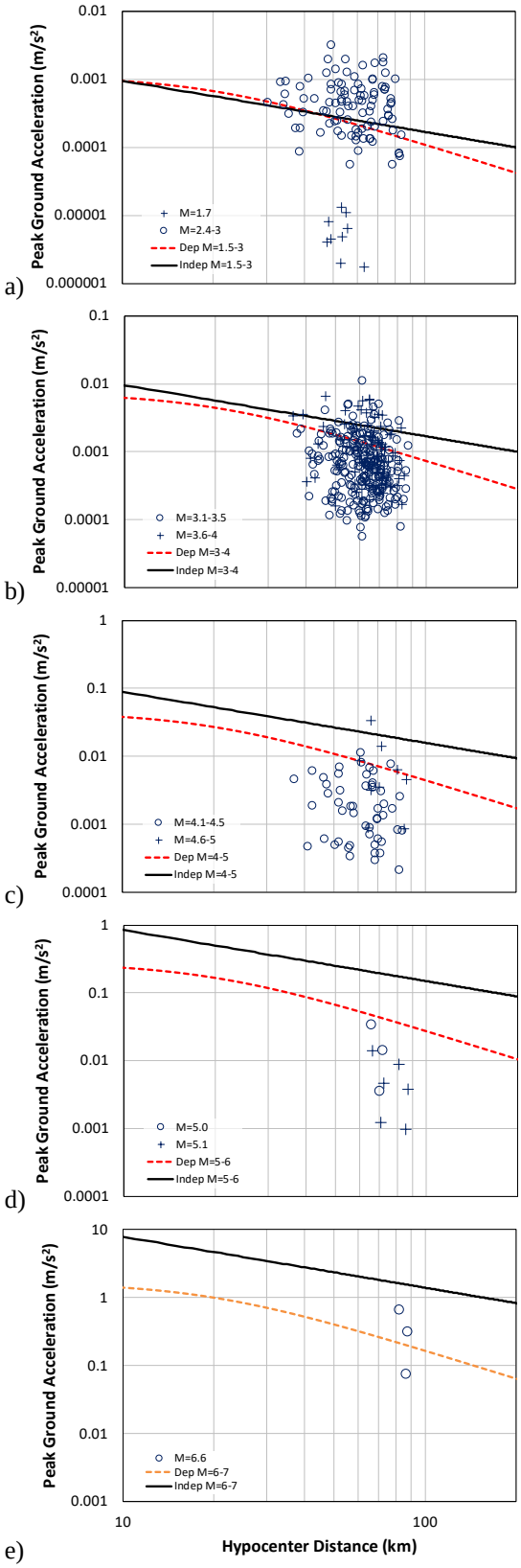


Fig.7 Comparison of GMPEresult to actual data: a) M=1.5-3.0, b) M=3.0-4.0, c) M=4.0-5.0, d) M=5.0-6.0, and e) M=6.0-7.0

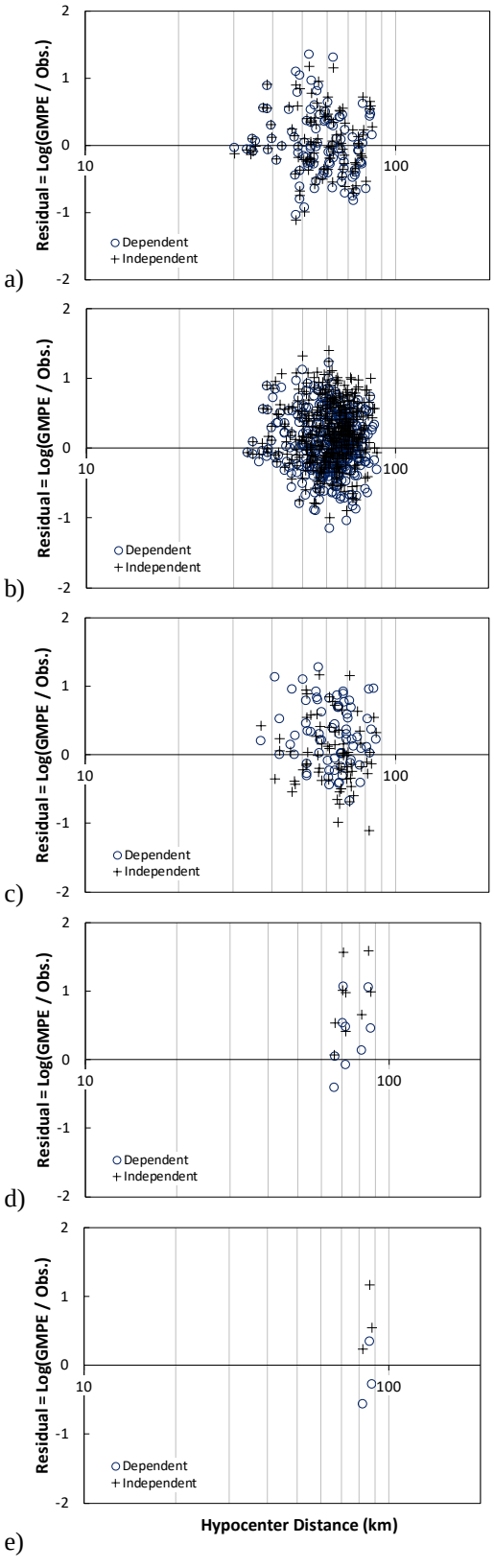


Fig.8 Residual analysis: a) M=1.5-3.0, b) M=3.0-4.0, c) M=4.0-5.0, d) M=5.0-6.0, and e) M=6.0-7.0

5. CONCLUSIONS

Central Sulawesi has very complex tectonic conditions. To understand better the earthquake hazard of the region, this study focused on the development of ground motion prediction equations based on broadband velocitymeter and strong motion accelerations recorded by instruments managed by BMKG temporarily since year 2015 and 2017. To examine further the accuracy of the equations, the seismicity declustering processes were performed by adopting the Reasenberg method; the declustering process reduced the number of dependent earthquake events of about a thousand to the number of independent mainshock events of about 400s. The site class of the instrument locations was SD.

The resulting expected geometric mean PGA from GMPE for dependent seismicity was similar to that for independent seismicity, except for higher magnitude earthquakes due to the limited number of data available. The GMPEs were examined further by comparing the expected PGAs with the actual PGA from earthquakes in the Sausu Fault region, including the damaging 29 May 2019 earthquake. Depending on the earthquake magnitude, the GMPEs may overestimate or underestimate the PGA values. Furthermore, the residual analyses were performed to examine trends of the expected PGA values.

This study is being extended to examine the effects earthquake mechanism (e.g., strike-slip, normal faulting, thrust faulting) on the GMPEs. This extension is intended primarily to reduce the model uncertainty. This study is also being extended to examine the acceleration response spectra for structures at different natural periods.

6. ACKNOWLEDGMENT

We would like to gratefully thank Indonesia Agency for Meteorology, Climatology, and Geophysics (BMKG), as well as Universitas Indonesia (through 2019 PhD Research Grant No NKB-0179/UN2.R3.1/HKP.05.00/2019) for their supports for this study.

7. REFERENCES

[1] PUSGEN, Indonesia Earthquake hazard map dan Source, ISBN 978-602-5489-01-3, 2017, pp.56-57.

[2] Gardner J. K. and Knopoff L., Is the sequence of earthquakes in Southern California, with aftershocksremoved, Poissonian?, Bull. Seis. Soc. Am., 64(5), 1974, pp.1363-1367.

[3] Reasenberg P., Second-order moment of central California seismicity, 1969-82, J. Geophys. Res., 90, 1985, pp.5479-5495.

[4] Uhrhammer R., Characteristics of Northern and Central California Seismicity, Earthquake Notes, 57(1), 1986, pp.21.

[5] Amini H., Comparing Reasenberg and Gruenthal Declustering Methods for North of Iran.Second European Conference on Earthquake Engineering and Seismology. 2014, pp.1-7.

[6] Savage W. U., Microearthquake Clustering near Fairview Peak, Nevada, and in the Nevada Seismic Zone,J. Geophys. Res., 77(35), 1972, pp.7049-7056.

[7] Molchan G. and Dmitrieva O., Aftershock identification: methods and new approaches, Geophys. J. Int.,109, 1992, pp.501-516.

[8] Knopoff L., The magnitude distribution of declustered earthquakes in southern California.Proc.Natl.Acad.Sci.USA,10.1073/pnas, 190241297, 2000, pp.11881-11884

[9] Sharma M.L., Douglas J., Bungum H., Kotadia J., Ground-Motion Prediction Equations Based On Data From The Himalayan And Zagros Regions, Journal Earthquake Engineering, 2008, pp.1-21.

[10] Pramono S., Prakoso W.A., Cummins P., Rahayu A., Rudyanto A., Syukur F., Sofian, Investigation of subsurface characteristics by using a V_{s30}parameter and a combination of HVSR and SPAC methods for microtremor arrays,IJTech Journal,2017, pp.983-992.

[11] Abrahamson N.A., Silva W.J., Kamai R., Summary of the ASK14 ground motion relation for active crustalk regions, Earthquake Spectra, 2014, pp.1025-1055.

Copyright © Int. J. of GEOMATE. All rights reserved, including the making of copies unless permission is obtained from the copyright proprietors.